

**Mechanical behaviors and phase transition of Ho<sub>2</sub>O<sub>3</sub> nanocrystals under high pressure**

Xiaozhi Yan, Xiangting Ren, Duanwei He, Bin Chen, and Wenge Yang

Citation: *Journal of Applied Physics* **116**, 033507 (2014); doi: 10.1063/1.4890341

View online: <http://dx.doi.org/10.1063/1.4890341>

View Table of Contents: <http://scitation.aip.org/content/aip/journal/jap/116/3?ver=pdfcov>

Published by the [AIP Publishing](#)

---

**Articles you may be interested in**

[High-pressure structural and elastic properties of Ti<sub>2</sub>O<sub>3</sub>](#)

*J. Appl. Phys.* **116**, 133521 (2014); 10.1063/1.4897241

[Strength and equation of state of fluorite phase CeO<sub>2</sub> under high pressure](#)

*J. Appl. Phys.* **112**, 013532 (2012); 10.1063/1.4736555

[Phase transformation of Ho<sub>2</sub>O<sub>3</sub> at high pressure](#)

*J. Appl. Phys.* **110**, 013526 (2011); 10.1063/1.3603027

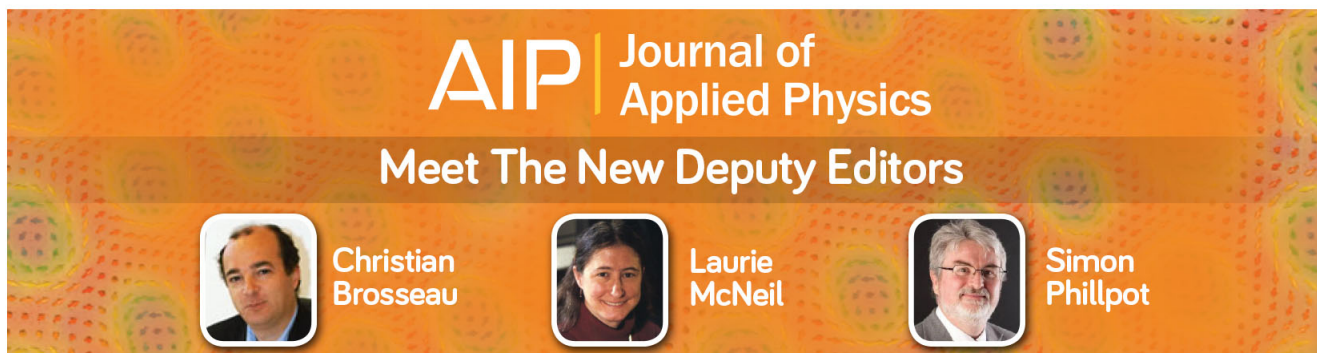
[High-pressure behavior of  \$\beta\$ -Ga<sub>2</sub>O<sub>3</sub> nanocrystals](#)

*J. Appl. Phys.* **107**, 033520 (2010); 10.1063/1.3296121

[High pressure phase transitions and compressibilities of Er<sub>2</sub>Zr<sub>2</sub>O<sub>7</sub> and Ho<sub>2</sub>Zr<sub>2</sub>O<sub>7</sub>](#)

*Appl. Phys. Lett.* **92**, 011909 (2008); 10.1063/1.2830832

---



**AIP** | Journal of Applied Physics

**Meet The New Deputy Editors**

	<b>Christian Brosseau</b>		<b>Laurie McNeil</b>		<b>Simon Phillpot</b>
---	---------------------------	---	----------------------	---	-----------------------

# Mechanical behaviors and phase transition of Ho<sub>2</sub>O<sub>3</sub> nanocrystals under high pressure

Xiaozhi Yan,<sup>1,2</sup> Xiangting Ren,<sup>1</sup> Duanwei He,<sup>1,3,a)</sup> Bin Chen,<sup>2</sup> and Wenge Yang<sup>2,4,a)</sup>

<sup>1</sup>Institute of Atomic and Molecular Physics, Sichuan University, Chengdu 610065, People's Republic of China

<sup>2</sup>Center for High Pressure Science and Technology Advanced Research (HPSTAR), 1690 Cailun Rd., Pudong, Shanghai 201203, People's Republic of China

<sup>3</sup>Institute of Fluid Physics and National Key Laboratory of Shockwave and Detonation Physics,

China Academy of Engineering Physics, Mianyang 621900, People's Republic of China

<sup>4</sup>High Pressure Synergetic Consortium (HPSynC), Geophysical Laboratory, Carnegie Institution of Washington, 9700 S Cass Avenue, Argonne, Illinois 60439, USA

(Received 7 May 2014; accepted 4 July 2014; published online 16 July 2014)

Mechanical properties and phase transition often show quite large crystal size dependent behavior, especially at nanoscale under high pressure. Here, we have investigated Ho<sub>2</sub>O<sub>3</sub> nanocrystals with *in-situ* x-ray diffraction and Raman spectroscopy under high pressure up to 33.5 GPa. When compared to the structural transition routine cubic → monoclinic → hexagonal phase in bulk Ho<sub>2</sub>O<sub>3</sub> under high pressure, the nano-sized Ho<sub>2</sub>O<sub>3</sub> shows a much higher onset transition pressure from cubic to monoclinic structure and followed by a pressure-induced-amorphization under compression. The detailed analysis on the  $Q$  ( $Q = 2\pi/d$ ) dependent bulk moduli reveals the nanosized Ho<sub>2</sub>O<sub>3</sub> particles consist of a clear higher compressible shell and a less compressible core. Insight into these phenomena shed lights on micro-mechanism studies of the mechanical behavior and phase evolution for nanomaterials under high pressure, in general. © 2014 AIP Publishing LLC. [<http://dx.doi.org/10.1063/1.4890341>]

## I. INTRODUCTION

Holmium oxide has been widely used in specialty catalysts, phosphors, laser materials,<sup>1</sup> and as a calibration standard material for optical spectrophotometers<sup>2</sup> due to sharp optical absorption peaks in the visible spectral range. Studying the influence of pressure on the structural stability and possible phase transition will provide us insight of the potential applications to extreme conditions. At ambient conditions, Ho<sub>2</sub>O<sub>3</sub> takes a cubic structure (C-type). Upon compression, it transforms to a monoclinic structure (B-type) at 8.9 GPa and a hexagonal structure (A-type) at 21.4 GPa in bulk form.<sup>3</sup> The nano-sized particles usually show more excellent performance related to the large surface fraction. So far, no results on the structural stability of Ho<sub>2</sub>O<sub>3</sub> nanocrystals in external stress environments have been reported. In this letter, we utilize the *in-situ* synchrotron x-ray diffraction and Raman spectroscopy methods on Ho<sub>2</sub>O<sub>3</sub> nanocrystals under high pressure up to 33.5 GPa and study the mechanical properties and phase transition route. The comparison with the properties of bulk sized Ho<sub>2</sub>O<sub>3</sub> provides an understanding of the crystal size effects on its physical properties, which is important not only for the fundamental science but also for further explorations of the industrial applications of this material.

## II. EXPERIMENTAL DETAILS

The nano-sized polycrystalline Ho<sub>2</sub>O<sub>3</sub> with purity of 99.9% (Beijing DK nano technology Co. LTD) was used as

the starting material. The sample was baked at 600 °C for 60 min to remove the possible hydroxide and moisture before loading into the diamond anvil cell. The x-ray diffraction confirmed the cubic structure at ambient condition, the same as the bulk Ho<sub>2</sub>O<sub>3</sub>.<sup>3</sup> Based on the Scherrer equation, the average particle size of the sample was estimated to be 14 nm, which is consistent with the SEM observation from the same sample source. A Mao-Bell type diamond anvil cell (DAC) with a pair of 300 μm culet sized diamond anvils was used to generate high pressure. The nano-Ho<sub>2</sub>O<sub>3</sub> powders with a small ruby chip were loaded into a 120-μm-diameter hole drilled in a stainless steel gasket. Silicone oil was used as the pressure-transmitting medium. The pressures were determined from the Ruby fluorescence shifts.<sup>4</sup>

The *in situ* high-pressure angle-dispersive x-ray diffraction (ADXRD) experiments were performed at the 4W2 beamline of the Beijing Synchrotron Radiation Facility (BSRF) with a wavelength of 0.6199 Å. The monochromatic x-ray beam was produced from a Si(111) monochromator and focused down to 21 μm (vertical) × 8 μm (horizontal) full-width at half-maximum (FWHM) by a pair of Kirkpatrick-Baez mirrors. The diffraction patterns at various pressures were recorded with a Mar345 imaging plate detector. High purity CeO<sub>2</sub> powder was used to calibrate the geometrical parameters of the detector. The collected 2D diffraction patterns were integrated into one-dimensional profiles with software FIT2D.<sup>5</sup>

The Raman spectrum measurements were also conducted at different pressures using a He/Ne-mixed ion laser with wavelength 633 nm to cover wave number range 50–1250 cm<sup>-1</sup>.

<sup>a)</sup>duanweihe@scu.edu.cn and yangwg@hpstar.ac.cn

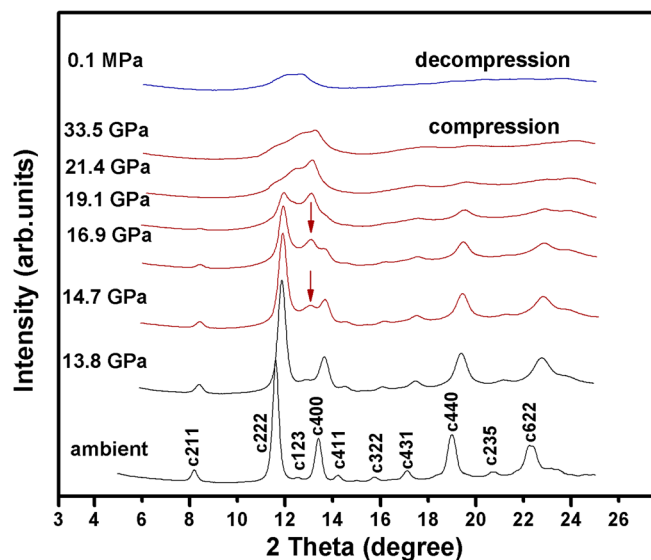


FIG. 1. Representative ADXD patterns of nano-crystalline  $\text{Ho}_2\text{O}_3$  under various pressures. The peaks labeled with red arrows are from the monoclinic phase.

### III. RESULTS AND DISCUSSION

The X-ray diffraction data are shown in Fig. 1 for both compression and decompression procedures. The highest pressure applied was 33.5 GPa. The cubic structure remains stable up to 14.7 GPa. Above 14.7 GPa, the intensity of a peak around  $13^\circ$  (labeled with red arrow in Figure 1) related to the high pressure monoclinic phase increases, indicating the phase transition begins. This transition pressure is about 6 GPa higher than that of the bulk counterpart.<sup>3</sup> The increased stability of the cubic phase in nanoscale  $\text{Ho}_2\text{O}_3$  was also confirmed by the Raman spectroscopy experiments. As shown in Fig. 2, all Raman modes of the cubic phase have blue shifts and broadening with increasing pressure. Above 15.1 GPa, the intensity of the peak at  $548.4\text{ cm}^{-1}$  (marked by an arrow in Fig. 2) increased drastically, indicating the onset of phase transition in nano- $\text{Ho}_2\text{O}_3$ .

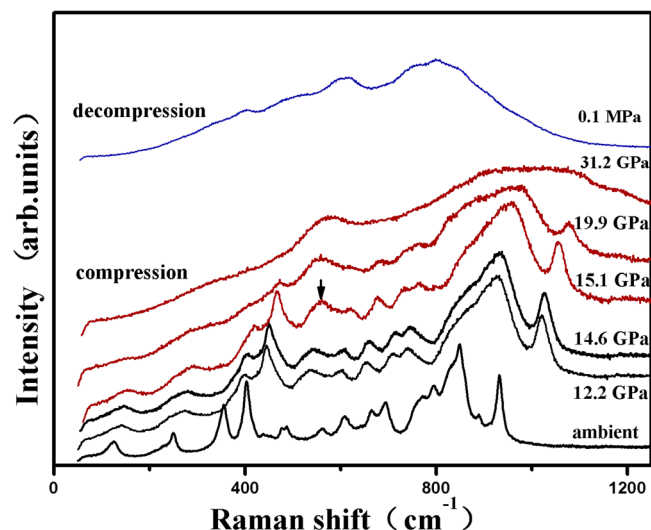


FIG. 2. Raman spectra of nano-crystalline  $\text{Ho}_2\text{O}_3$  under various pressures. The arrow indicates the onset of the high pressure phase.

The nano-size effect on the structural stability remains debated.<sup>6–11</sup> Some materials show higher phase transition pressures with decreasing particle size,<sup>7,9,12</sup> while others exhibit the opposite dependence.<sup>13</sup> The competition of larger surface area and limited density of storage defect may play important role for different systems. Defects can be annealed out more easily in nano-crystals than in extended solids, for instances, the dislocations can easily slip to surface in a nano-crystal. Thus, it is generally believed that nanoparticles smaller than a critical size (typically 10–30 nm) are defect free.<sup>14</sup> The deviatoric strains measured from nano- $\text{Ho}_2\text{O}_3$  and its bulk counterpart with x-ray diffraction analysis at ambient pressure were  $(-0.012 \pm 0.018)\%$  and  $(0.107 \pm 0.0103)\%$ , respectively, which confirms that  $\text{Ho}_2\text{O}_3$  nanocrystalline is nearly defect free, while the bulk  $\text{Ho}_2\text{O}_3$  remains nearly 10 times higher deviatoric strain contributed by much higher defect density. The phase transition usually starts from the defected region. For our case, the nearly defect free  $\text{Ho}_2\text{O}_3$  nanocrystalline requires a higher pressure to provide sufficient driving force to initiate the phase transition compared with its bulk counterparts. This observation is consistent with the reported results for other solid state phase transitions induced by temperature as well.<sup>15</sup> In addition, the higher surface energy in nano-crystals may also contribute to the elevation in phase transition pressure.<sup>16</sup>

Upon further compression, peak broadening increases, indicating that the sample becomes progressively more disordered in the high pressure monoclinic phase, as shown in Fig. 1. Above 21.4 GPa, all diffraction peaks disappeared, left with one broad, amorphous peak between  $10^\circ$  and  $14^\circ$ . The crystalline structure of the sample completely transformed into an amorphous state. The broad peak shifts to higher angles with further increasing pressure and lower angles upon decompression to ambient pressure. The pressure-induced-amorphization (PIA) was confirmed by the Raman spectroscopy measurements as well (Fig. 2). At 31.2 GPa, only two broad peaks can be observed. The decompressed sample also has only a few broad Raman peaks. The consistency between the XRD and Raman results confirms the occurrence of PIA in the  $\text{Ho}_2\text{O}_3$  nanocrystals. Upon decompression to ambient pressure, both the XRD and Raman patterns show some differences to the patterns at the highest pressure, which indicates a phase transition from the high density amorphous phase at high pressure to a low density amorphous phase at ambient pressure. Further high energy pair distribution function (PDF) study is needed to compare these two structures in detail.

One may raise the question: why the PIA occurs in the nano-sized  $\text{Ho}_2\text{O}_3$  rather to transfer to a hexagonal phase in the bulk sized  $\text{Ho}_2\text{O}_3$ . For many PIA cases, the parent low pressure phase could be connected to the high pressure phase through a displacive path. The PIA happens when the energy barrier needs to be overcome from the frustration of the parent metastable crystalline phase in transforming to the high-pressure equilibrium phase, especially at low and room temperature.<sup>17,18</sup> For the case of bulk  $\text{Ho}_2\text{O}_3$ , the above mentioned displacive path does exist between monoclinic phase and hexagonal phase of  $\text{Ho}_2\text{O}_3$  between 14.8 GPa and 26.4 GPa.<sup>3</sup>

For nano-crystalline  $\text{Ho}_2\text{O}_3$ , the surface fraction accounts for a significant portion for the physical property

and structural stability. One needs an effective way to distinguish the surface contribution from the bulk.<sup>19</sup> Proposed by Palosz *et al.*,<sup>27</sup> for nano-particles, the diffraction intensity at large  $Q$  ( $= 2\pi/d$ ) is mainly from the grain core, while the diffraction intensity at low  $Q$  is mainly contributed by the surface of grains. Therefore, diffraction peaks observed at large  $Q$  could be used to characterize the lattice parameter from the grain core, while the small  $Q$  ones are sensitive to the lattice of the surface of the grains, which was named “apparent lattice parameter.” For the low pressure cubic phase, we can derive the unit cell volumes of core and shell (surface) part of the grains from the “apparent lattice parameter” at high  $Q$  and low  $Q$  values, respectively. This concept has been successfully used to analyze the compression behavior of nano-sized nickel powder under high pressure.<sup>28</sup> Following the third-order Birch-Murnaghan equation of state (EoS):<sup>25,26</sup>

$$P = 1.5K \left[ \left( \frac{V}{V_0} \right)^{\frac{2}{3}} - \left( \frac{V}{V_0} \right)^{\frac{5}{3}} \right] \times \left\{ \left\{ 1 - 0.75(4 - K') \left[ \left( \frac{V}{V_0} \right)^{\frac{2}{3}} - 1 \right] \right\} \right\}. \quad (1)$$

One can calculate the bulk modulus of the materials. Here,  $V/V_0$  is the reduction ratio of unit cell volume at pressure  $P$  comparing to ambient pressure.  $K$  is the bulk modulus, and  $K'$  is the pressure derivative of bulk modulus. Three reflections at  $Q = 1.44 \text{ \AA}^{-1}$ ,  $2.05 \text{ \AA}^{-1}$ , and  $2.37 \text{ \AA}^{-1}$  were chosen for the bulk moduli calculations for the pressure range from ambient to 14 GPa, while the nano- $\text{Ho}_2\text{O}_3$  stayed at pure low pressure phase. The EoS obtained from these  $Q$  vectors is plotted in Fig. 3(b) and the corresponding bulk moduli are calculated from Eq. (1). Comparing to the bulk modulus for the bulk  $\text{Ho}_2\text{O}_3$  at 206 GPa, modulus at low  $Q = 1.44 \text{ \AA}^{-1}$  is 20% lower (164.1 GPa), while the bulk modulus at the high  $Q = 2.37 \text{ \AA}^{-1}$  is 10% larger (221 GPa). The  $Q$ -dependent bulk moduli indicate that the surface shell (high  $Q$ ) is more compressible than the core (low  $Q$ ) of the grains. A similar soft shell—hard core system in nanocrystalline iron was reported with high pressure Mössbauer spectroscopy study.<sup>29</sup>

We also conduct the regular Rietveld refinements on each pressure diffraction pattern with the entire  $Q$  range with best fitting, which compromise the high  $Q$  and low  $Q$  values. The result yields bulk modulus 186.4 GPa, nearly a 10% decreasing from the bulk count part. But a close look on the GSAS Rietveld refinement shows the direct evidence of the lattice variation as a function of  $Q$  value. Fig. 4 shows the refined result on the ambient pressure diffraction data. Overall the calculated profile matches the experimental data pretty well ( $R_p = 1.2\%$ ). But the systematic deviation tendency is clear: at low  $Q$ , the measured intensities shift to lower- $Q$  side, while at high  $Q$ , the measured data shift to higher- $Q$  side. As the GSAS fitting pattern is an average of the diffraction intensity of both the nanoparticle core and shell, this tendency of shift reflects the tensiled shell and the compressed core in the nano-crystalline  $\text{Ho}_2\text{O}_3$ . So the regular GSAS refinement will yield an averaged result, which may largely depend on the portions of contribution from core to shell.

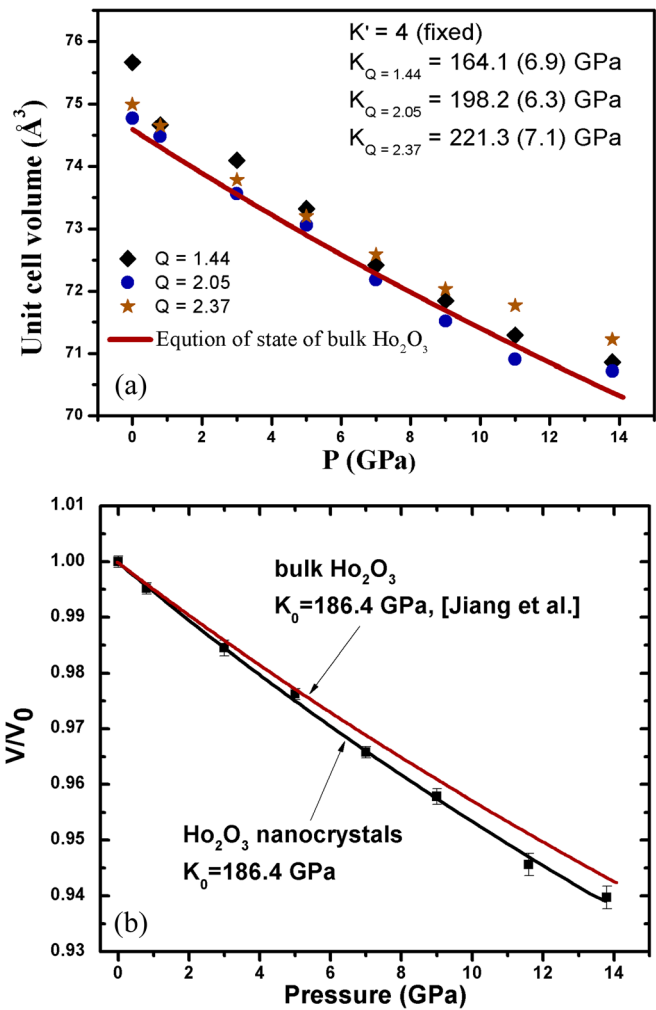


FIG. 3. Comparison of the equation of state of nano-crystalline and bulk-sized  $\text{Ho}_2\text{O}_3$ . The  $Q$ -dependent (a) and overall (b) unit cell volume of nano- and bulk- $\text{Ho}_2\text{O}_3$  cubic phase up to 14 GPa. Fitting the  $V$ - $P$  data using Eq. (1) with the third-order Birch-Murnaghan equation of state yield different bulk moduli as shown in the figures.

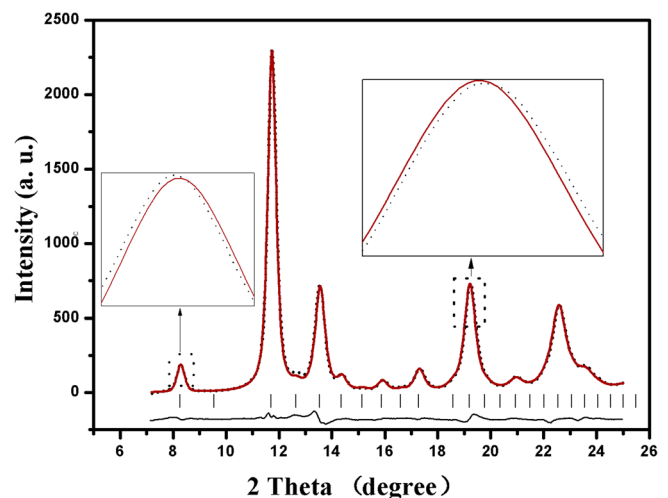


FIG. 4. Powder x-ray diffraction structure refinement of 14 nm-sized  $\text{Ho}_2\text{O}_3$  at ambient pressure. The insets are the zoom-in views of the selected peaks. (Black dotted line: measured pattern; red line: calculated pattern; black tick: position of peaks; line below tick: difference between calculated and measured patterns).

The compressibility on nano-materials under high pressure has been reported with higher bulk modulus for Fe<sub>2</sub>O<sub>3</sub> and Si cases,<sup>20,21</sup> but lower with PbS and CdSe cases,<sup>22,23</sup> or no significant difference especially in relative low pressure region.<sup>24</sup> Considering the different mechanical responses from these surfaces/interface regions and core part of nanoparticles under high pressure, one may consider to utilize the method demonstrated above to diagnose the core and shell contributions. In our case with average 14 nm particle size, the enhanced overall compressibility of nano-crystalline Ho<sub>2</sub>O<sub>3</sub> is mainly due to the higher compressibility of the surface shell. We believe with increasing the particle size, the surface effect will play less contribution, and the bulk modulus increases towards to the bulk one. The apparent lattice parameter approach provides a very useful way to evaluate the mechanical property of core-shell composite nano-crystals.

#### IV. SUMMARY

In summary, the phase transition and compressibility of Ho<sub>2</sub>O<sub>3</sub> nano-crystals with average grain size 14 nm were investigated at pressure up to 33.5 GPa under quasi-hydrostatic conditions with synchrotron x-ray diffraction and Raman spectroscopy. The onset transition pressure in Ho<sub>2</sub>O<sub>3</sub> nano-crystals from cubic to monoclinic phase is 6 GPa higher than that in the bulk counterpart, which suggests the structural stability of the cubic phase is enhanced by the nano-scaled grain size. The Ho<sub>2</sub>O<sub>3</sub> nano-crystals do not transform to the hexagonal phase as the bulk Ho<sub>2</sub>O<sub>3</sub>, but to an amorphous state upon further compression and to another amorphous form upon decompression, which provides an effective method to make amorphous form nano-Ho<sub>2</sub>O<sub>3</sub> by pressure. In the pressure range up to 13.8 GPa, the averaged bulk modulus of Ho<sub>2</sub>O<sub>3</sub> nano-crystals is 186.4 ± 8.1 GPa, which is about 10% lower than the reported values for bulk Ho<sub>2</sub>O<sub>3</sub>. The analysis on the Q dependence of the bulk moduli indicates that the enhanced overall compressibility of nano-crystalline Ho<sub>2</sub>O<sub>3</sub> is a consequence of the higher compressibility of the surface shells of the nano-crystals.

#### ACKNOWLEDGMENTS

This work was supported by the China 973 Program (Grant No. 2011CB808200) and National Natural Science Foundation of China (Grant No. 11027405). W.Y.

acknowledges the support from EFree, an Energy Frontier Research Center supported by DOE-BES under Award No. DE-SC0001057.

- <sup>1</sup>J. C. Travis, J. C. Zwinkels, F. Mercader, A. Ruíz, E. A. Early, M. V. Smith, M. Noël, and M. Maley, *Anal. Chem.* **74**, 3408 (2002).
- <sup>2</sup>R. P. MacDonald, *Clin. Chem.* **10**, 1117 (1964).
- <sup>3</sup>S. Jiang, J. Liu, X. Li, L. Bai, W. Xiao, Y. Zhang, C. Lin, Y. Li, and L. Tang, *J. Appl. Phys.* **110**, 013526 (2011).
- <sup>4</sup>H. K. Mao, J. Xu, and P. M. Bell, *J. Geophys. Res.* **91**, 4673, doi:10.1029/JB091iB05p04673 (1986).
- <sup>5</sup>A. P. Hammersley, S. O. Svensson, M. Hanflanda, A. N. Fitcha, and D. Haus, *High Press. Res.* **14**, 235 (1996).
- <sup>6</sup>C. C. Chen, A. B. Herhold, C. S. Johnson, and A. P. Alivisatos, *Science* **276**, 398 (1997).
- <sup>7</sup>J. Z. Jiang, L. Gerward, D. Frost, R. Secco, J. Peyronneau, and J. S. Olsen, *J. Appl. Phys.* **86**, 6608 (1999).
- <sup>8</sup>B. Chen, D. Penwell, M. B. Kruger, A. F. Yue, and B. Fultz, *J. Appl. Phys.* **89**, 4794 (2001).
- <sup>9</sup>S. B. Qadri, E. F. Skelton, A. D. Dinsmore, J. Z. Hu, W. J. Kim, C. Nelson, and B. R. Ratna, *J. Appl. Phys.* **89**, 115 (2001).
- <sup>10</sup>B. Chen, D. Penwell, and M. B. Kruger, *Solid State Commun.* **115**, 191 (2000).
- <sup>11</sup>C. Moffitt, B. Chen, D. M. Wieliczka, and M. B. Kruger, *Solid State Commun.* **116**, 631 (2000).
- <sup>12</sup>J. Z. Jiang, J. S. Olsen, L. Gerward, D. Frost, and D. Rubie, *Europhys. Lett.* **50**, 48 (2000).
- <sup>13</sup>Z. Wang, S. K. Saxena, V. Pischedda, H. P. Liermann, and C. S. Zha, *Phys. Rev. B.* **64**, 012102 (2001).
- <sup>14</sup>R. L. Penn and J. F. Banfield, *Science* **281**, 969 (1998).
- <sup>15</sup>Y. Mnyukh, *Am. J. Condens. Matter Phys.* **3**, 89 (2013).
- <sup>16</sup>K. Jacobs, D. Zaziski, E. C. Scher, A. B. Herhold, and A. P. Alivisatos, *Science* **293**, 1083 (2001).
- <sup>17</sup>S. K. Sikka, *J. Phys.: Condens. Matter* **16**, S1033 (2004).
- <sup>18</sup>S. M. Sharma and S. K. Sikka, *Prog. Mater. Sci.* **40**, 1 (1996).
- <sup>19</sup>H. Gleiter, *Prog. Mater. Sci.* **33**, 223 (1989).
- <sup>20</sup>J. Z. Jiang, J. S. Olsen, L. Gerward, and S. Morup, *Europhys. Lett.* **44**, 620 (1998).
- <sup>21</sup>Y. J. Wang, J. Zhang, J. Wu, J. L. Coffey, Z. Lin, S. V. Sinogeikin, W. Yang, and Y. Zhao, *Nano Lett.* **8**, 2891 (2008).
- <sup>22</sup>S. B. Qadri, J. Yang, B. R. Ratna, E. F. Skelton, and J. Z. Hu, *Appl. Phys. Lett.* **69**, 2205 (1996).
- <sup>23</sup>S. H. Tolbert and A. P. Alivisatos, *Annu. Rev. Phys. Chem.* **46**, 595 (1995).
- <sup>24</sup>S. Fernando, M. Baynes, B. Chen, J. F. Banfield, and H. Zhang, *RSC Adv.* **2**, 6768 (2012).
- <sup>25</sup>F. Birch, *J. Geophys. Res.* **83**(B3), 1257, doi:10.1029/JB083iB03p01257 (1978).
- <sup>26</sup>R. J. Angel, M. Bujak, J. Zhao, G. D. Gatta, and S. D. Jacobson, *J. Appl. Crystallogr.* **40**, 26 (2007).
- <sup>27</sup>B. Palosz, E. Grzanka, S. Gierlotka, S. Stel'makh, R. Pielaszek, U. Bismayer, J. Neuefeind, H. P. Weber, and W. Palosz, *Acta Phys. Pol. A* **102**, 57 (2002).
- <sup>28</sup>J. Zhang, Y. Zhao, and B. Palosz, *Appl. Phys. Lett.* **90**, 043112 (2007).
- <sup>29</sup>S. Trapp, C. T. Limbach, U. Gonser, S. J. Campbell, and H. Gleiter, *Phys. Rev. Lett.* **75**, 3760 (1995).